

Analysis Of Electromagnetic Field On Transmission Line To Human Using Infinite Element Method

Bambang Suprianto, Munoto, Aditya Dwinugraha

Abstract—The use of high voltage is not only to reduce power losses but also to produce electromagnetic field near the transmission line. This electromagnetic field is harmful to humans near the transmission line. In this paper, analysis of the distribution of electromagnetic field were presented by using simulation based on finite element method (FEM). The basic principle of FEM was to divide the structure, the body, or the observed area to be finite element. The transmission line of 500 kV and its effect to the operators working near the transmission line were simulated to obtain the electromagnetic field distribution.

Index Terms—Transmission line, electromagnetic field, operator, finite element method.

I. INTRODUCTION

Electric power is one of the most useful energy in daily activities. The electric power is generated from various power plants, such as water turbine generator, steam turbine generator, gas turbine generator, etc. The output voltage of generator is increased by step-up power transformer and transferred to transmission line. The use of high voltage on transmission system will reduce the power losses and the voltage drop. This high voltage is then decreased by step-down power transformer in power distribution system.

The use of high voltage on transmission line also produce the electromagnetic field [1,11,12]. This electromagnetic field endangers to the human, such as operators and residents near transmission line.

In this study, the distribution of electromagnetic field on transmission line was investigated by using simulation based on finite element method (FEM) [2,5,15,18]. The transmission line of 500 kV was analyzed its electromagnetic field. This would provide how much influence of the electromagnetic field to operators.

II. ELECTROMAGNETIC FIELD CALCULATION ON TRANSMISSION LINE

In electromagnetic field calculation, intensity of electromagnetic field (H) is associated with density of electromagnetic field (B), $B = \mu H$. The equation of Helmholtz can be seen in (1) [5]. For the system frequency is 50 Hz, electromagnetic field is modeled as current equation law as defined below:

Bambang Suprianto, Universitas Negeri Surabaya, Department of Electrical Engineering, Indonesia
Munoto, Universitas Negeri Surabaya, Department of Electrical Engineering, Indonesia
Aditya Dwinugraha, Institut Teknologi Sepuluh Nopember, Department of Electrical Engineering, Indonesia

$$\frac{\partial^2 H}{\partial x^2} + \frac{\partial^2 H}{\partial y^2} + \frac{\partial^2 H}{\partial z^2} - \epsilon \mu \frac{\partial^2 H}{\partial t^2} - \mu \sigma \frac{\partial H}{\partial t} = 0 \quad (1)$$

with μ is magnet permeability, σ is conductivity, and ϵ is dielectric permeability contant.

By considering time harmonics system, $H = H e^{j\omega t}$, the equation become:

$$\frac{\partial^2 H}{\partial x^2} = -\omega^2 H \quad \text{and} \quad \frac{\partial H}{\partial t} = j\omega H \quad (2)$$

with ω is angular frequency.

The equation is then simplified as:

$$\nabla^2 H - j\omega \sigma \mu H + \omega^2 \epsilon \mu H = 0 \quad (3)$$

By regarding to three dimensions (x,y,z), so that:

$$\frac{\partial}{\partial x} \left(\frac{\partial H}{\partial x} \right) + \frac{\partial}{\partial y} \left(\frac{\partial H}{\partial y} \right) + \frac{\partial}{\partial z} \left(\frac{\partial H}{\partial z} \right) - (j\omega \mu \sigma - \mu \epsilon \omega^2) H = 0 \quad (4)$$

III. SIMULATION METHOD

A. Finite Element Method (FEM)

Finite element method (FEM) is one of the numeric methods mostly used to solve problems of structure, thermal, and electromagnetic. In this method, the problems were finished by using basic principle of discretion process. The process of discretion on finite element was division process on object structure modeling into the infinite small elements [1,2,20,21]. Those elements were small meshes of the object. The calculation method was to calculate the small meshes that would be combined into a larger form to be joined. The obtained results were sourced from the continue estimation value to the what was associated with mesh parts, so that the expected form was obtained [5,8,23,25].

B. Electromagnetic Field Calculation on Transmission Line

General method of electromagnetic field calculation near transmission line could be calculated by using analysis of two dimensions, in which the transmission line was assumed to be parallel with flat earth surface. The coordinate system could be explained as depicted on Fig. 1. The conductor of transmission line was parallel with Z axis. The current flowing on the conductor, I_z , was opposite with Z axis.

The direction of electromagnetic field intensity at x_j, y_j with distance from earth surface, r_{ij} , had amplitudo as:

$$H_{ji} = \frac{I_i}{2\pi r_{ij}} \quad (5)$$

In vector notation, the equation could be written as:

$$H_{ji} = \frac{I_i \times r_{ji}}{2\pi r_{ji}^2} = \frac{I_i}{2\pi r_{ji}} \Phi_{ij} \quad (6)$$

For unit of direction vector, Φ_{ij} , the equation became:

$$H_{ji} = -\frac{y_i - y_j}{r_{ij}} u_x + \frac{x_i - x_j}{r_{ij}} u_y \quad (7)$$

with u_x was direction vector unit paralld with X axis and u_y was direction vector unit paralld with Y axis.

If there were some conductors carrying the current, the total of electromagnetic field intensity could be defined as:

$$H_{ji} = \sum \frac{I_i}{2\pi r_{ji}} \Phi_{ij} \quad (8)$$

The electromagnetic field near three-phases transmission line was affected by earth return, especially for far point from the transmission line (and near earth). For transmission in balance condition, this current was distributed through earth along the transmission line although the current total would be zero in the end. The earth current is calculated by using Carson's equation. Therefore, the intensity of electromagnetic field produced by transmission line and earth current could be written as below [6]:

$$H_{ji} = \frac{I_i}{2\pi r_{ij}} \Phi_{ij} - \frac{I_i}{2\pi r'_{ij}} \left[1 + \frac{1}{3} \left(\frac{2}{\gamma r'_{ij}} \right)^4 \right] \Phi'_{ij} \quad (9)$$

(8) showed the electromagnetic field due to transmission effect, while (9) showed the electromagnetic field due to earth current which was also a correction factor because the earth current as:

$$\gamma = [j\omega\mu(\sigma + j\omega\epsilon)]^{1/4} \quad (10)$$

with σ was earth conductivity (0.001 – 0.002 S/m), ϵ was earth permittivity earth (8.85.10⁻¹² equal with air permittivity

$$r'_{ij} = [(x_i - x_j)^2 + (y_i - y_j + 2/\gamma)^2]^{1/4} \quad (11)$$

$$\Phi'_{ij} = -\left[\frac{y_i - y_j + 2/\gamma}{r'_{ij}} \right] u_x + \frac{x_i - x_j}{r'_{ij}} u_y \quad (12)$$

(11) and (12) were shown that if the earth current effect was considered, the intensity of electromagnetic field would not be in the same phase with the current source.

C. Calculation of Field and Unification of Triangle Element

The main principle of finite element method was discrete which was formation of small triangle elements of mesh with unlimited amount, as depicted on Fig. 2 and 3. By knowing the potential value (V) on the one triangle element, the value of electromagnetic field on insulator surface was obtained.

The equation of energy on electrostatic field for each element could be obtained as follow:

$$W_E = \frac{1}{2} \epsilon_0 \epsilon_r V^T S V \quad (13)$$

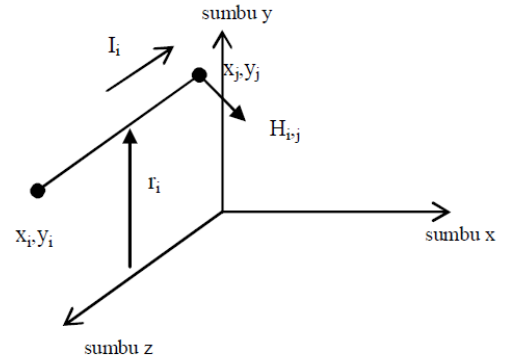


Figure 1. Coordinate system of calculation.

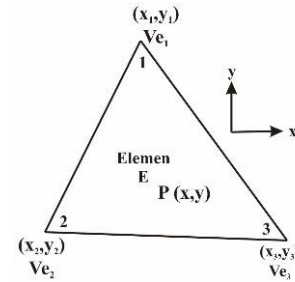


Figure 2. Modeling of triangle element.

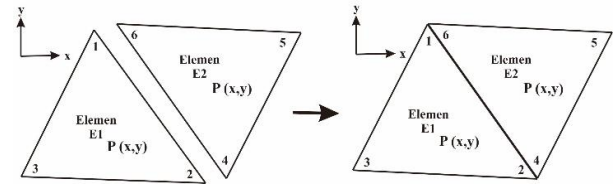


Figure 3. Combining of two triangle elements.

Based on the combining of some elements, the value of energy could then be calculated as follow

$$W = \frac{1}{2} \epsilon_0 \epsilon_r V_{con}^T S V_{con} \quad (14)$$

$$S = C^T S_{dis} C \quad (15)$$

(15) could be outlined into a coefficient matrix which was connected between one triangle with the others, as below:

$$S = \begin{bmatrix} S_{11}^{(1)} + S_{66}^{(2)} & S_{12}^{(1)} + S_{64}^{(2)} & S_{13}^{(1)} & S_{65}^{(2)} \\ S_{21}^{(1)} + S_{46}^{(2)} & S_{22}^{(1)} + S_{44}^{(2)} & S_{23}^{(1)} & S_{45}^{(2)} \\ S_{31}^{(1)} & S_{32}^{(1)} & S_{33}^{(1)} & 0 \\ S_{56}^{(1)} & S_{54}^{(1)} & 0 & S_{55}^{(2)} \end{bmatrix} \quad (16)$$

D. Modeling of Tower, Insulator, and Human

In the beginning, the transmission tower was modeled. The chosen tower type was suspension tower as shown in Fig. 4. Secondly, insulator of 500 kV was modeled as depicted on Fig. 5. The modeling of conductor bar used epoxy resin material, as seen in Fig. 6. Later, the insulator fins with polyimide material and end fitting with iron

material were installed. The insulator was then mounted to insulator suspension as shown in Fig. 7. The human was modeled as seen in Fig. 8.

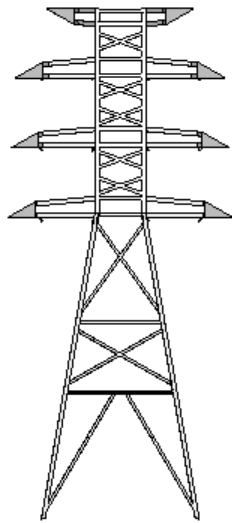


Figure 4. Modeling of transmission tower.



Figure 5. Modeling of conductor bar on insulator.



Figure 6. Modeling of insulator.

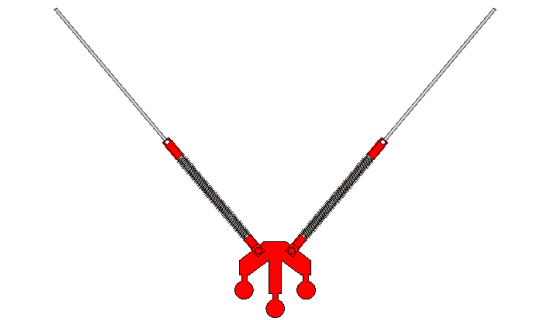


Figure 7. Modeling of insulator with suspension.



Figure 8. Modeling of human.

E. Material of Transmission Tower, Polymer Insulator, and Human

The materials of transmission tower and polymer insulator used in simulation were explained in Table 1. The material of insulator could be seen in Table 2, while the material of human was shown in Table 3.

Table1: Material Datasheet Of Transmission Tower And Conductor

Unit	Material	
	Copper (Pure)	Ferro A6M (lossy)
Epsilon	1	5.9
Mue	1	1
El. Cond. (S/m)	5.96×10^7	
Therm. Cond. (W/K/m)		2

Table 2. Material Datasheet Of Insulator

Unit	Material	
	Epoxy Resin	Polymide (lossy)
Epsilon	4	3.5
Mue	1	1
El. Cond. (S/m)	1×10^{-15}	
Rho (kg/m ³)	1500	1400
Therm. Cond. (W/K/m)	0.2	0.2
Heat cap. (kJ/K/kg)		1
Diffusivity (m ² /s)		1.42857×10^{-7}
Young's Mod. (GPa)	13	2.5
Poiss. Ratio	0.45	0.4
Thermal Exp. (1e ⁻⁶ /K)		25

Table 3: Material Datasheet Of Human

Unit	Material (Heart)
Epsilon	1
Mue	1
Rho (kg/m ³)	1100
Therm. Cond. (W/K/m)	0.293
Heat cap. (kJ/K/kg)	3.5
Diffusivity (m ² /s)	7.61039×10^{-8}
Bloodflow (W/K/m ³)	9100
Metab. Rate (W/m ³)	1620

F. Transmission Line Simulation

The simulated transmission line had the rated voltage of 500 kV, as depicted on Fig. 9. The three-phases voltage of 500 kV was applied to the red conductor in Fig. 9 with the placement of R, S, and T.

IV. RESULT AND ANALYSIS

A. Transmission Line Simulation

The distribution of electromagnetic field on transmission line was shown in Fig. 10. The red colour in Fig. 10 showed the electromagnetic field with the highest value, while the blue colour in Fig. 10 presented the lowest value of the electromagnetic field. The value of electromagnetic field distribution in the middle of transmission line was seen in Fig. 10(a) and (b).

B. Electromagnetic Field on Transmission Tower

The value of electromagnetic field on the tower experienced the fluctuations, as depicted on Fig. 11. In the beginning, this value was increased constantly. The significant increase occurred at point of 23, in which the highest value was obtained at the altitude of 39.31 m, that was 0.83 Vs/m^2 , and the lowest value was presented at point of 60.

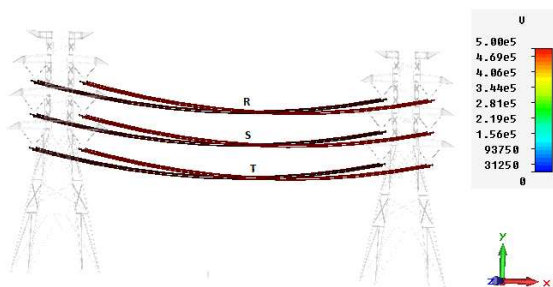
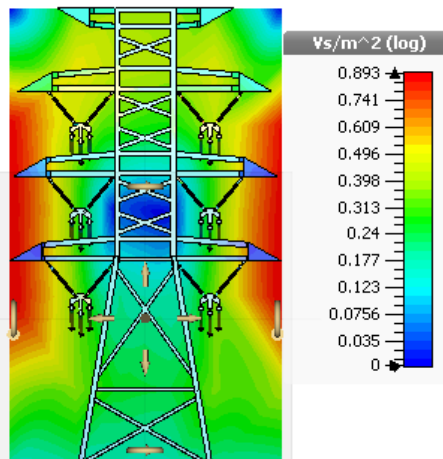


Figure 9. Rated voltage of the simulated transmission line.



(a)

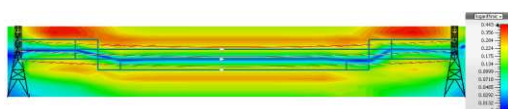


Figure 10. Distribution of electromagnetic field on transmission line: a) Front view. b) Side view

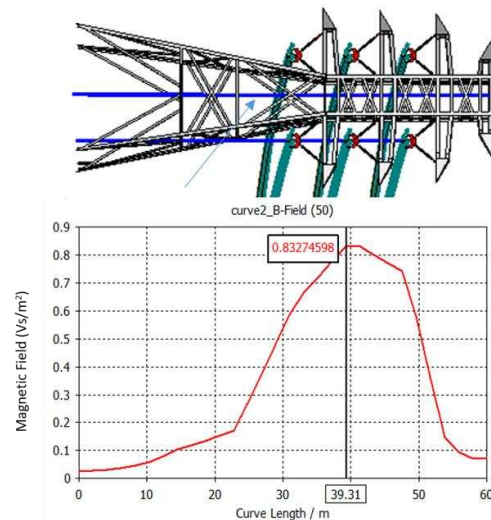


Figure 11. Curve of electromagnetic field based on the transmission line.

C. Electromagnetic Field on The Three Phases

The value of electromagnetic field on T phase of transmission line at high of 30 m was obtained as depicted on Fig. 12. The blue line presented the peak value of the curve. The electromagnetic field value at point of T was 0.17 Vs/m^2 and experienced an increase until point of R. The point of S with altitude of 38 m had 0.21 Vs/m^2 , while the point of R with altitude of 46 m had 0.35 Vs/m^2 .

D. Electromagnetic Field on The Conductor

The value of electromagnetic field on the conductor of transmission line experienced an increase and a lowly decrease. Fig. 13 showed that the curve line at 0-2.2 m was slightly increased with the electromagnetic field mean value of 0.025 Vs/m^2 and the curve line at 10 m was significantly increased until the curve line reached 23 m with 0.328 Vs/m^2 . The decrease on the conductor was obtained because the greatest electromagnetic field was near the conductor (the electromagnetic field in the conductor was lower than near the conductor). Fig. 14 explained the electromagnetic field on human, that was 0.0187 Vs/m^2 .

E. Comparison of Electromagnetic Field on Human Under Transmission Line

The comparison was conducted for each distance of 30 m along transmission line. The value of electromagnetic field at zero distance from tower was increased until at distance of 120 m, as depicted on Fig. 14. The values was then almost constant until at distance of 180 m with 0.06 Vs/m^2 . This showed that the greatest value of electromagnetic field was 0.06 Vs/m^2 in the middle of transmission line or under conductor (the lowest distance).

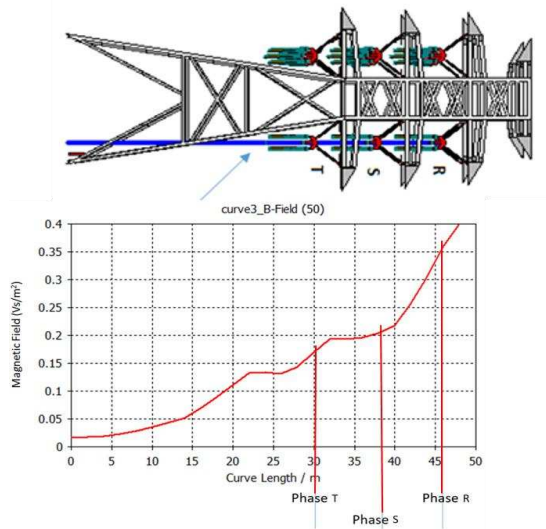


Figure 12. Curve of electromagnetic field on R, S, and T.

F. Comparison of Direct Measurement and Simulation Result

The measurement was conducted on transmission line of 500 kV located in Krian-Gresik, West of Surabaya. The measurement used *ELF Field Strength Measurement System*, HI-3604. Firstly, the distance was measured and adjusted to the distance in simulation. Later, the values of electromagnetic field between the direct measurement and the simulation were compared as seen in Table 4.

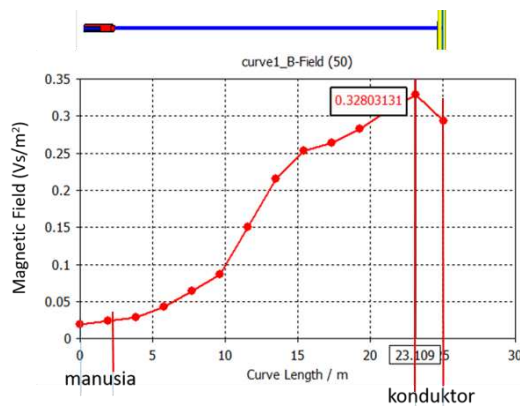


Figure 13. Comparison of electromagnetic field on the insulator fins with crack.

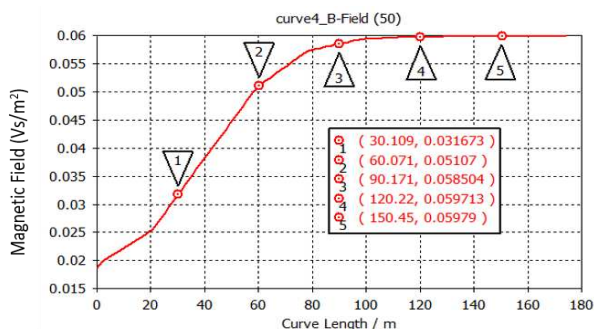


Figure 14. Comparison of electromagnetic field on the insulator fins with crack

Table 4: The Comparison Results

Distance (m)	Simulation Result (Vs/m ²)	Measurement Result (Vs/m ²)
0	0.018	0.02
30	0.031	0.035
60	0.051	0.038
90	0.058	0.034
120	0.059	0.048
150	0.059	0.043
180	0.06	0.05

V. CONCLUSION

The highest value of electromagnetic field on transmission line was located in left side and right side of transmission line, that was 0.83 Vs/m², whereas the lowest value was located on the human under conductor, that was 0.0187 Vs/m². It was caused by the material type and material thermal conductivity which led to the polarization effect between macroscopic interface and decreased the dielectric properties. Steel material on transmission line had the higher value than the other.

Based on the simulation to human under transmission line, the mean value was obtained as 0.048 Vs/m². It indicated that the human near the transmission tower exceeded the safe limit (the safe limit for human was 0.025 Vs/m² based on SNI 04-6950-2003).

The comparison result between the simulation and the direct measurement was not much different. The highest value of electromagnetic field was located at altitude of 180 m in the middle transmission line or right below the conductor with the lowest distance, that was 0.06 Vs/m² based on the simulation and 0.05 Vs/m² based on the measurement.

REFERENCES

- [1] Tobing, Bonggas L., "Basic High Voltage Testing Technique," Jakarta: PT Gramedia Pustaka Utama, Indonesia, 2003.
- [2] Vassiliki T. Kontargyri, Ioannis F. Gonos, Ioannis A. Stathopoulos, and Alex M. Michaelides, "Simulation of the Electric Field on High Voltage Insulators using the Finite Element Method", IEEE 2006.
- [3] Sani Ugustra, "Study of Electric Field on Vertical Configuration of 150kV Transmission Channel", Indonesia, 2015.
- [4] SPLN 121, "High Voltage Air Channel Construction 70 KV and 150KV with Concrete Pill / Steel", Jakarta, 1996.
- [5] Bunmat A., P.Pao-la-or, "Analysis of Magnetic Field Effects Operators Working a Power Transmission Line Using 3D Finite Element Method", Thailand, 2015.
- [6] Hitoshi Kusuma Putra, "Analysis of Effect of Isolator Field on Distribution Tower When Affected by High Voltage by Using Finite Element Method", Institut Teknologi Sepuluh Nopember, Indonesia, 2016.
- [7] Hayt William H. And John A. Buck, "Electro magnetics Seventh Edition", Penerbit Erlangga, Indonesia, Januari 2006.
- [8] Yusrizal Afif, "Analysis of Electric Field Distribution on Insulator Polymer Material Hanging Using Finite Element Method", Institut Teknologi Sepuluh November, Indonesia, 2014.
- [9] I Made Yulistya Negara, "Principles High Voltage Technique and Practical Applications", Graha Ilmu, Surabaya, Indonesia, 2013.
- [10] Irwan Prasetyo, "Analysis of Electric Field and Magnetic Field at Operation Planning of 150 kV SUTT Peraan-Ubud", Universitas Udayana, Bali, Indonesia, 2004.
- [11] Suwino dan Fri Murdiyah, "Study of Magnetic Field and Electric Field on High Voltage Air Channel (SUTT) 150 kV Kampar-Pekanbaru Based on Recommendations IRPA / INIRC WHO", Universitas Riau, Indonesia, 2010.

- [12] Essa-J-Abdul Zehra, Mahmoud Moghavvemi, Maher M. I. Hashim and Kashem, Muttaqi, *Network Reconfiguration Using PSAT for Loss Reduction in Distribution Systems*, 1st International Conference on Energy, Power and Control (EPC-IQ), College of Engineering, University of Basrah, Iraq, 2010, 62-66.
- [13] L.Ramesh, S.Ravindiran, S.P.Chowdhury, S.Chowdhury, Y.H.Song and P.K.Goswami, *Distribution System Loss Minimization and Planning using Cymdist*, 42nd International Universities Power Engineering Conference (UPEC), University of Brighton, Brighton, UK, 2007, 316-321.
- [14] Arefi Ali , Haghifam Mahmood-reza, Yavartalab Akbar, Olamaei Javad and Keshtkar Hessam, *Loss reduction planning in electric distribution networks of IRAN until 2025*, 16th conference on Electric Power Distribution Network (EPDC), Bandar Abbas , Iran, 2011, 1-6.
- [15] Yang Lin and Guo Zhizhong, *Reconfiguration of Electric Distribution Networks for Energy Losses Reduction*, 3rd International conference on Electric Utility Deregulation and Restructuring and Power Technologies (DRPT), Nanjing, China, 2008, 662-667.
- [16] Juan Carlos Olivares, Yilu Liu and Jose M. Cañedo, *Reducing Losses in Distribution Transformer*, IEEE transactions on power delivery, 18(3), July 2003, 821-826.
- [17] Dong Zhang, Zhengcai Fu, and Liuchun Zhang, *Joint Optimization for Power Loss Reduction in Distribution Systems*, IEEE transaction on Power Systems, 23(1), 2008, 161-169.
- [18] R. Srinivasa Rao, *An Hybrid Approach for Loss Reduction in Distribution Systems using Harmony Search Algorithm*, International Journal of Electrical and Electronics Engineering, 2010, 462- 467.
- [19] Sameer S. Mustafa., Mohammed H. Yasen, Hussein H. Abdullah and Hadi K. Hazaa, *Evaluation of Electric Energy Losses in Kirkuk Distribution Electric System Area*, Iraq J. Electrical and Electronic Engineering, 7(2), 2011, 144-150.
- [20] Thomas Nippert, Kathrin Steinke, Martin Schrors, *Loss Reduction in High Voltage Urban Distribution Systems*, 19th International conference on Electricity Distribution, session 3, Vienna, Austria, Paper No. 719, 2007, 1-4.
- [21] Best practices in distribution loss reduction: reference book, *Power Development Department (PDD)*, J&K, Jammu, 2007.
- [22] Flávio V. Gomes, Sandoval Carneiro Jr., Jose Luiz R. Pereira, Marcio P. Vinagre., Paul Augusto N. Garcia, Edimar J. Oliveira and Leandro R. Araujo, *A New Distribution System Reconfiguration Approach Using Optimal Power Flow Technique and Sensitivity Analysis for Loss Reduction*, Panel Session: Advanced Models for Distribution System Analysis, IEEE PES General Meeting San Francisco, CA, USA, 1, 2005, 897-901.
- [23] M.V. Deshpande, *Electrical Power System Design* (New Delhi: TATA McGraw-Hill Publishing Company Limited).
- [24] B.R.Gupta, *Power System Analysis and Design* (New Delhi: S. Chand & Company Limited).
- [25] V.K. Mehta and R. Mehta, *Principles of Power System* (New Delhi: S. Chand & Company Limited, 2008).
- [26] B.L. Theraja, and A.K. Theraja, *A textbook of electrical technology, Transmission, distribution and utilization in SI system of units, volume III* (New Delhi: S. Chand & Company Limited, 2005)